

THESIS FOR THE DEGREE OF LICENTIATE OF PHILOSOPHY

Variation Simulation Customized for  
Composites by Including FEM  
Simulations of Orthotropic Lamina

Cornelia Jareteg

**CHALMERS**



**GÖTEBORGS UNIVERSITET**

Department of Mathematical Sciences  
Division of Mathematics  
Chalmers University of Technology and University of Gothenburg  
Gothenburg, Sweden 2015

Variation Simulation Customized for Composites by Including FEM Simulations of Orthotropic Lamina  
Cornelia Jareteg

© Cornelia Jareteg, 2015

Department of Mathematical Sciences  
Division of Mathematics  
Chalmers University of Technology and University of Gothenburg  
SE-412 96 Gothenburg  
Sweden  
Telephone +46 (0)31 772 1000

Fraunhofer-Chalmers Research Centre for Industrial Mathematics  
Chalmers Science Park  
SE-412 88 Gothenburg  
Sweden

Typeset with L<sup>A</sup>T<sub>E</sub>X.  
Printed in Gothenburg, Sweden 2015

## Abstract

The use of composite materials is increasing in many fields of production. Composite manufacturing, as well as other fields of production, suffers from uncertainties resulting in products that deviate from the specification. Geometry assurance is a common procedure used to keep the variations in product assemblies under control. However, the methods used to simulate the variation are not developed for composites. In this thesis, two methods are presented that address typical uncertainties within composite production.

The method presented in Paper I focuses on the variation of fiber orientation and ply thickness within fibrous laminae. Variation simulation for the fiber orientation and ply thickness parameters is combined with a traditional such method. The combined variation simulation is carried out so that it is possible to study the effects of including perturbations in these composite parameters.

In Paper II, a method that captures a special type of deviation common for composites, called spring-in, is presented. These deviations are seen especially in T-beam structures and occur during the curing step of production, i.e., hardening in an oven. A FEM thermal expansion simulation is performed on the anisotropic composite laminate as a part of the traditional variation simulation method. The curing temperature is one parameter, along with the standard geometric parameters, within the proposed method.

The two methods proposed are tested on subassemblies originating from automotive and aviation industry, respectively. Applying the method presented in Paper I to the test case gives a resulting variation where the variance is increased by a factor of 10%. No structural differences are seen. Hence, these results indicate that traditional variation simulation is sufficient with the inclusion of a correction factor for composites. The method presented in Paper II is a new contribution to the field of geometry assurance. In addition, the results show an increase by a factor 4 in the resulting variation for the test case between keeping the curing temperature fixed at nominal value and letting it vary.

**Keywords:** Geometry assurance, FEM, Composites, Shell model, Process variation, Method of Influence Coefficients, Monte Carlo, Orthotropic material, Manufacturing, Tolerance analysis, Variation simulation, Spring-in



## Acknowledgements

I would like to thank my supervisors Prof. Stig Larsson at Chalmers and Assoc. Prof. Fredrik Edelvik at FCC for their support and guidance through this work. Further, I want to address a special thanks to Dr. Christoffer Cromvik at FCC who have encouraged me and engaged in my work with a lot of time and effort.

Thanks also to Assoc. Prof. Kristina Wärmefjord, Prof. Rikard Söderberg and Assoc. Prof. Lars Lindkvist at PPU, Chalmers for pursuing this project, as well as for the support and the good discussions.

Thanks to Dr. Samuel Lorin who have patiently explained things to me whenever I have asked, and to Erik Svenning for the valuable support during the startup of this project. A great thanks to all my colleagues, at the department of Computational Engineering at FCC, for the pleasant discussions in the corridor.

Finally, thank you Klas for your endless love and support, and for always being by my, and our daughter Noomi's, side.

This research has received funding from the European Union's Seventh Framework Programme (FP7/2007-2013) under grant agreement n°314003 and from the Wingquist Laboratory VINN Excellence Centre, financed by the Swedish Governmental Agency for Innovation Systems (VINNOVA).

Cornelia Jareteg  
Gothenburg, April 2015



## List of Papers

The licentiate thesis includes the following papers.

- I. **C. Jareteg**, K. Wärmefjord, R. Söderberg, L. Lindkvist, J. Carlson, C. Cromvik, F. Edelvik (2014). Variation simulation for composite parts and assemblies including variation in fiber orientation and thickness. *Procedia CIRP Conference on Assembly Technologies and Systems*, **23**, pp 235-240, doi:10.1016/j.procir.2014.10.069.
- II. **C. Jareteg**, K. Wärmefjord, C. Cromvik, R. Söderberg, L. Lindkvist, J. Carlson, S. Larsson, F. Edelvik (2014). Geometry assurance integrating process variation with simulation of spring-in for composite parts and assemblies. *Procedia ASME International Mechanical Engineering Congress & Exposition*.



# Nomenclature

## Abbreviations

CFRP	Carbon Fiber Reinforced Polymer
CTE	Coefficients of Thermal Expansion
dof	degree of freedom
FE	Finite Element
FEM	Finite Element Method
LSL	Lower Specification Limit
MC	Monte Carlo
MIC	Method of Influence Coefficients
RMS	Root Mean Square
USL	Upper Specification Limit

## Geometry assurance

$(x, y, z)$	Point in $\mathbb{R}^3$
$\alpha$	Geometric direction
$\mu$	Mean value of normal distribution
$\sigma$	Standard deviation of normal distribution
$M$	Number of Monte Carlo iterations
$N$	Number of FE nodes
$n_{\text{tol}}$	Number of input parameters to the variation simulation

$t$  Displacement  
 $v$  Direction vector of locator  
 $A1, A2, A3, B1, B2, C1$  Locators, i.e., points in locating scheme

### Geometry assurance, sub- and superscripts

$i$  FE node no  
 $k$  Monte Carlo iteration no

### Finite element method

$(\xi, \eta, \zeta)$  Point in unit cube  
 $(x_1, x_2, x_3)$  Point in  $\mathbb{R}^3$   
 $\epsilon$  Strain tensor  
 $\sigma$  Stress tensor  
 $\delta$  Dirac delta  
 $\Gamma$  Boundary of geometry domain  
 $\mathcal{S}$  Trial space  
 $\mathcal{V}$  Test space  
 $\mathbf{D}$  Matrix of elastic coefficients  
 $\mathbf{e}$  Basis vector  
 $\mathbf{f}$  Body force vector  
 $\mathbf{h}$  Surface force vector, traction vector  
 $\mathbf{I}$  Identity matrix  
 $\mathbf{J}$  Jacobi matrix  
 $\mathbf{n}$  Normal vector  
 $\mathbf{p}$  Point in  $\mathbb{R}^3$   
 $\mathbf{q}$  Point in  $\mathbb{R}^3$   
 $\mathbf{T}$  Transformation matrix

$\mathbf{U}$	Displacement of point in shell reference surface
$\mathbf{u}$	Displacement
$\mathbf{v}$	Interior part of $\mathbf{u}$
$\mathbf{w}$	Test function
$\mathbf{X}$	Point in shell reference surface
$\mathbf{x}$	Point in the FE shell
$\bar{\mathbf{u}}$	Displacement of director
$\bar{\mathbf{x}}$	Director
$\nu$	Poisson's ratio
$\Omega$	Geometry domain of solid continuous body
$\theta$	Rotation of the director
$\varphi$	Test function
$c$	elastic coefficient
$d$	Number of space dimensions
$E$	Young's modulus
$G$	Shear modulus
$g$	Prescribed boundary displacement
$h$	Prescribed traction
$I$	Index set
$n$	Normal
$N^A$	Finite element shape function for node $A$
$n_{\text{en}}$	Number of element nodes
$n_{\text{eq}}$	Number of finite element equations
$s$	Tensor, general nonsymmetric
$t$	Tensor, general symmetric
$z^A$	Thickness function in node $A$

**Finite element, sub- and superscripts**

$\alpha, \beta, \gamma, \lambda$  Subscript index assumed to belong to  $\{1, 2\}$  unless otherwise stated

$A$  Superscript denoting FE node

$h$  Superscript denoting discrete function or set

$i, j, l, k$  Subscript index assumed to belong to  $\{1, 2, 3\}$ , unless otherwise stated

$l$  Superscript denoting lamina coordinates





# Contents

<b>Abstract</b>	<b>iii</b>
<b>Acknowledgements</b>	<b>v</b>
<b>List of Papers</b>	<b>vii</b>
<b>Nomenclature</b>	<b>ix</b>
<b>1 Introduction</b>	<b>1</b>
1.1 Product and production development . . . . .	1
1.2 Problem description . . . . .	3
1.3 The mathematics of this problem . . . . .	3
<b>2 Geometry assurance</b>	<b>5</b>
2.1 Locating schemes . . . . .	5
2.2 Input and output parameters with tolerances . . . . .	7
2.3 Variation simulation . . . . .	8
2.3.1 Monte Carlo . . . . .	9
2.3.2 MIC - method of influence coefficients . . . . .	10
2.4 Measures of variation . . . . .	11

<b>3</b>	<b>A brief introduction to composites</b>	<b>13</b>
3.1	Materials . . . . .	13
3.2	Production processes . . . . .	14
3.3	Uncertainties in composite production . . . . .	15
3.3.1	Ply thickness and fiber orientation . . . . .	15
3.3.2	Spring-in phenomena . . . . .	15
<b>4</b>	<b>FEM for composite shells</b>	<b>17</b>
4.1	Solid elements . . . . .	18
4.2	Shell model . . . . .	25
4.3	Composite shells . . . . .	29
4.3.1	Orthotropic material models . . . . .	29
4.3.2	Laminae of orthotropic materials . . . . .	32
<b>5</b>	<b>Summary of papers</b>	<b>33</b>
5.1	Paper I: Variation simulation for composite parts and assemblies including variation in fiber orientation and thickness . . . . .	33
5.1.1	Method . . . . .	34
5.1.2	Test case . . . . .	35
5.1.3	Results . . . . .	36
5.2	Paper II: Geometry assurance integrating process variation with simulation of spring-in for composite parts and assemblies . . .	36
5.2.1	Method . . . . .	37
5.2.2	Test case . . . . .	37
5.2.3	Results . . . . .	38
	<b>Bibliography</b>	<b>41</b>

# Chapter 1

## Introduction

A short description of the field of application is presented (Section 1.1), followed by a specification of the focus of interests within this field (Section 1.2). Research previously done related to the focus problem is mentioned to understand the context. The mathematical parts is then emphasized (Section 1.3).

### 1.1 Product and production development

In manufacturing industry design, quality, durability and cost are important factors. The problem is that no production process is perfect, e.g., there are variations and deviations from specifications. Hence there must be strategies on how to deal with this. Geometric errors of this kind need to be kept under control and specifications need to be met. The concept of geometry assurance is further described in Chapter 2. Understanding and knowledge of geometric variation will help to keep the cost low while maintaining good product quality. Therefore, to develop a rewarding production process, it is crucial to have realistic informative simulation tools.

The manufacturing process can be divided into three phases, see the product realization loop in Figure 1.1:

- **The concept phase** where the design of the product and the production process are formulated by means of virtual simulations. In this phase it is possible to test and easily evaluate a number of different concepts using the virtual simulation tool.

- **The verification phase** in which smaller batches with prototypes are produced and evaluated along with the virtual simulation results.
- **The production phase** where product and production process specifications are established and the real production with larger batches are started. Real measurements are still made to control the process and they are also compared with simulation results in order to improve the simulation tool for later purposes.

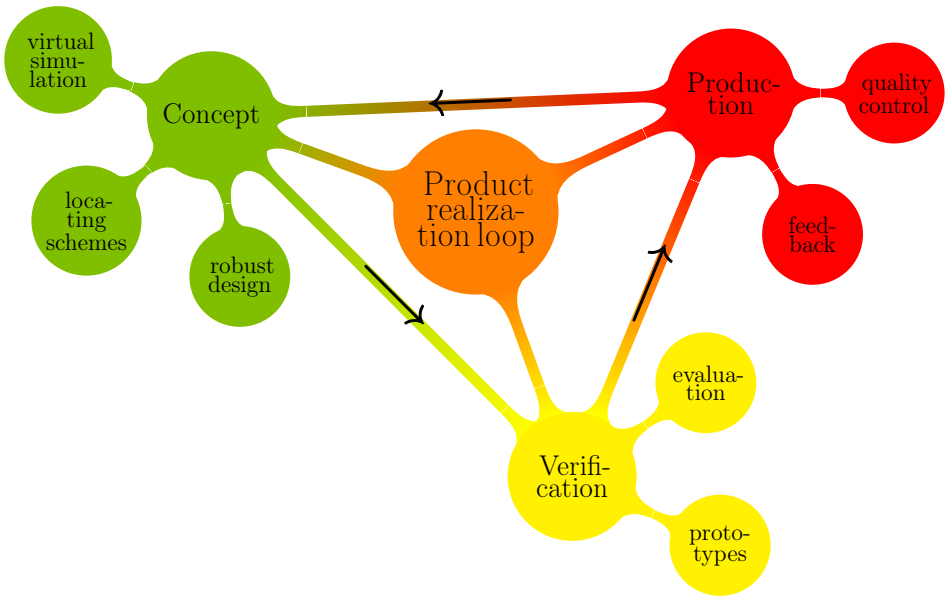


Figure 1.1: The three main phases of the manufacturing process described by the product realization loop.

There may be conflicting goals between design of the product and the required precision of the production process. A design that is insensitive to variation is desired. A robust design concept allows for some production process variations while the product still meets the requirements. In contrast, in a non robust design concept variations need to be kept very low otherwise requirements will not be fulfilled. Demanding small variations is in most cases possible but very expensive and hence not desirable.

## 1.2 Problem description

Usage of composite materials in manufacturing industries, such as aviation and automotive industry, is increasing. Evaluation of the applicability of existing virtual simulation tools on composite materials is therefore needed. Further, it may then be necessary to modify the models or develop new models customized for composites.

A lot of research has been done in the field of variation simulation, for both metallic and plastic parts. A comprehensive review is given in [10]. In addition much research has been carried out on the mechanics of composites and their production processes. A review of this field is found in [7]. Simulation of parts of composite production processes have also been done, see e.g. [6]. However, these fields of research, variation simulation and composite simulations, need to be studied in combination. Research about integration of composite production process simulations into the field of variation simulations will help to improve many manufacturing processes.

The two appended papers treat two aspects of the inclusion of composite specific features in geometry assurance. First, the effect of variation in fiber orientation and ply thickness of the composite material is studied in Paper I. Secondly, a method where process variation, occurring in the completion phase of composite production, is integrated into traditional variation simulation. The method is developed, tested and evaluated in Paper II.

## 1.3 The mathematics of this problem

Variation simulation is the theoretic tool within geometry assurance giving the opportunity to test features in a virtual factory and understand how the geometric variation on single parts propagates through production and affects the final product assembly. This is a typical problem within the field of uncertainty quantification.

In variation simulation parts are considered as rigid or compliant. In both appended papers only compliant geometries are used. Compliant geometries are discretized using finite element meshes and the deformation occurring during the assembly process is solved using the finite element method (FEM). Parts are often thin and hence modeled by shell elements. Thin composite parts are modeled by layered orthotropic shell elements. For the composites, it is also possible to use layered solid elements, i.e., wedge or hexahedral elements.

The Monte Carlo (MC) method is used to perform the variation simulations. Further, some basic statistics is used in the analysis of the results from simulations.

The combination of the FEM and the MC method is computationally demanding and give very long simulation times. Therefore, to reduce simulation time a model reduction is applied via the method of influence coefficients (MIC), [16], further described in Section 2.3.2.

# Chapter 2

## Geometry assurance

The term Geometry assurance is used for the process of keeping variation in production assemblies under control to guarantee a final product with good quality.

In manufacturing industry, products are produced by joining together parts or subassemblies into larger assemblies that constitute the finished product. A door of a car, or a wing of an aircraft, are typical such finished products where geometry assurance is applicable.

The geometry assurance procedure starts with the choice of a suitable locating scheme (Section 2.1) for the parts and subassemblies. Then input parameters and tolerances for them are defined (Section 2.2). Next variation simulation is performed (Section 2.3) to simulate how the assembly process deforms the parts causing them to deviate from specification. The simulation results are analyzed and the defined tolerances are examined using, e.g., the root mean square (RMS) as a measure of variation (Section 2.4). If needed, adjustments are made and the simulation is rerun until a satisfying result is reached.

### 2.1 Locating schemes

When the parts of a product are assembled during production they need to be kept locked in fixtures while joined together. These fixtures have different designs and functionality. In the simulations we model the fixture by allocating scheme. Except for locking the part in space, a locating scheme should con-

tribute to a robust design concept. The design concept includes the choice of locating system, the design of the geometry of the parts, the choice of materials etc. A robust design concept suppresses variation, i.e., small errors in e.g. part geometry or fixture give small resulting variations in the assembly. The opposite of a robust design concept is a sensitive design concept, where small errors are amplified giving large resulting variations.

Robustness is only one parameter influencing the choice of locating scheme. Certain practical factors may also be important to consider. In [17] it is shown how to find the optimal locating scheme with respect to robustness. An extensive discussion on how to choose a suitable locating scheme in general is given in [27].

A rigid part has 6 degrees of freedom (*dof*) in space, 3 translations and 3 rotations. All degrees of freedom need to be locked by the locating scheme so that the part is fixed in space. To lock all dof, 6 points, at which the part is locked from movement in one direction, is defined. These 6 points are called the *main locators*. So, to define a locating scheme we need to specify 6 points together with a direction vector for each point. One main difference between different types of locating schemes is whether these direction vectors are orthogonal or not. The most common types of locating schemes include:

- **The 3-2-1 locating scheme** consists of three groups of points and direction vectors, see Figure 2.1. First, the A-group consists of three points, A1, A2 and A3, with equal direction vectors,  $v_A$ . Second, the B-group include two points, B1 and B2 having direction vector  $v_B$  orthogonal to  $v_A$ . Finally the C-group consists of one point, C1, with direction vector  $v_C$  orthogonal to both  $v_A$  and  $v_B$ . By the A-points, the part is prevented from movement in the translation dof equal to  $v_A$  as well as two rotation dof. The B-points prevent movement in the translation dof equal to  $v_B$  and one rotation dof. The C-point prevent the part from moving in the final translation dof equal to  $v_C$ .
- **The 3-point locating scheme** is a special case of the 3-2-1 locating scheme. The points and direction vectors are defined in the same way with the only difference that A1=B1=C1 and A2=B2.
- **The 3-direction locating scheme** is a locating scheme where the direction vector need not be orthogonal. It is defined in the same way as the 3-2-1 locating scheme, but the condition that  $v_A$ ,  $v_B$  and  $v_C$  are orthogonal is removed.
- **The 6-direction locating scheme** is another non-orthogonal locating scheme, see Figure 2.2. In this locating scheme the locators are not

grouped as in the preceding since all six points ( $D_1, \dots, D_6$ ), have different direction vectors that need not be orthogonal to each other.

Note that when defining a non-orthogonal locating scheme, such as the 3-direction or 6-direction locating schemes, caution need to be taken to not end up with a part that is still free to move in some dof.

For compliant parts these locating schemes might need to be extended by adding some extra support points.

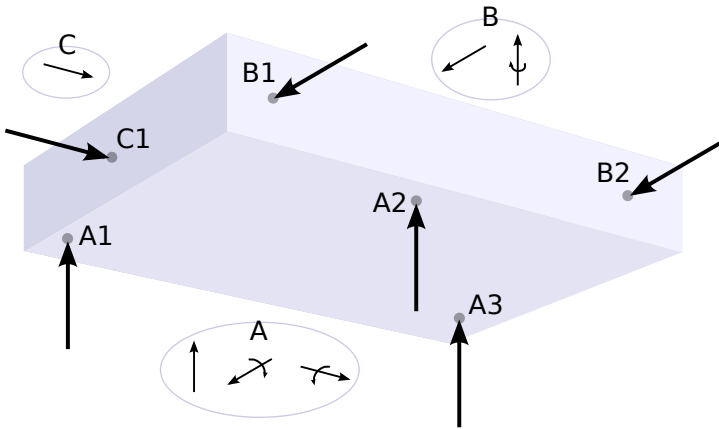


Figure 2.1: 3-2-1 locating scheme.

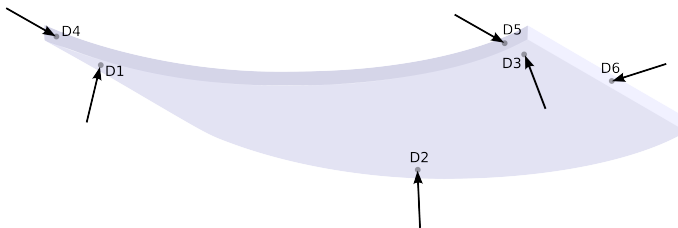


Figure 2.2: 6-direction locating scheme.

## 2.2 Input and output parameters with tolerances

In practice, parts are non-nominal, i.e., the geometry deviates from the specification. The fixtures holding the parts also have deviations. Further, there

are uncertainties in process parameters. The real sources of variation are many and may even be impossible to describe or specify completely by parameters. Instead, those parameters that are selected are said to represent the sources of variation. They are adjusted accordingly by e.g. tuning their magnitude. Input parameters commonly defined are:

- Displacement of locators.
- Displacement of joining points.
- Displacement of contact points.
- Process parameters; e.g., fiber orientation, ply thickness, curing temperature.

For each input parameter a tolerance is specified, i.e., an upper and a lower specification limit (USL and LSL). The tolerances may have a large effect on the variation depending on how robust the design concept is. Smaller tolerances give smaller variation. However, smaller tolerances are more expensive because the production needs to be more precise. A well chosen locating scheme may allow for looser tolerances which keeps costs low.

As output parameters from a variation simulation we get:

- The displacement of each finite element (FE) node in each direction in each MC iteration, i.e., the variation in each FE node.
- The displacement in predefined measures, e.g., the displacement of a certain point or the relative displacement between two points on different parts of the assembly.

## 2.3 Variation simulation

The term variation simulation here refers to the virtual assembly procedure of a product. There are three main objectives commonly seen within variation simulation [32]:

- **Tolerance allocation/synthesis:** How should tolerances be distributed to individual parts with the requirement that the final assembly meets specifications?

- **Tolerance optimization:** How could manufacturing costs be decreased but still assure that assemblies are within specifications?
- **Tolerance analysis/accumulation:** How does part tolerances accumulate and affect the final assembly?

Often these objectives more or less coincide and may be hard to distinguish between in the analysis of a case.

Before the non-rigid variation simulation can be carried out, the case to be simulated need to be specified. This is done by the following steps, where items in *italic* are not always needed:

1. Define the FE mesh for all the compliant parts.
2. Choose a locating scheme and specify the locators for each part.
3. Specify the joining points.
4. *Specify the contact points/surfaces.*
5. *Define the process parameters.*
6. Specify the tolerances for each input parameter.
7. *Define the measures where variation is of special interest.*

After this set up, variation simulation can be carried out using e.g. the Monte Carlo (MC) method (Section 2.3.1). The MC method, used here, is one of two common approaches to variation simulation. Deterministic methods, often based on Taylor expansion, constitutes the other common approach.

For the variation simulations performed, the Monte Carlo based software and research tool RD&T is used, [25]. Examples of other software products where variation simulation is implemented are 3DCS [1] and VSA [29].

When the MC method is used together with the FEM (discussed in Chapter 4), simulation time gets indefensibly long even for small problems and geometries. To overcome this issue the method of influence coefficients (MIC) is introduced (Section 2.3.2).

### 2.3.1 Monte Carlo

In simulations using the Monte Carlo method a random variable is defined for each input parameter. In the following, we assume independent, normally

distributed random variables. Given the tolerances for each input parameter we choose the mean value,  $\mu$ , and standard deviation,  $\sigma$ , for the random variables to be

$$\mu = \frac{1}{2}(\text{USL} + \text{LSL}) \quad (2.1)$$

$$\sigma = \frac{1}{6}(\text{USL} - \text{LSL}) \quad (2.2)$$

The quantity  $6\sigma$  is commonly used in production industry as the specification interval value [22]. This gives 99.7% of the samples within specification limits. For an even higher percentage being within limits,  $8\sigma$  is also frequently used.

When a value for each input parameter has been sampled, the assembly process is simulated. As output, we get the resulting displacement in each finite element node or predefined measure. To get accurate results, this is repeated a large number of times. So, one variation simulation consists of a number of Monte Carlo iterations.

### 2.3.2 MIC - method of influence coefficients

The method of influence coefficients (MIC) is presented in [16] and it is applied to shorten simulation time significantly. A linear behavior is assumed making the MIC valid for small deformation problems.

In this method, solutions to the finite element problem are precomputed for certain input settings. These solutions are then stored in a matrix and used as a basis. From this basis a new solution can be computed very fast by matrix vector multiplication instead of solving the complete finite element problem again. Since the MC method requires a finite element solution in each iteration, the gain in simulation time is multiplied by the number of MC iterations.

To set up the basis of solutions each input parameter is perturbed by a unit displacement one at a time. Each unit perturbed parameter results in a vector with displacements for all finite element nodes. These vectors make up the columns of the basis. Hence, for  $n_{\text{tol}}$  input parameters, the matrix of precomputed solutions, i.e., the basis, will be of size  $N \times n_{\text{tol}}$ , where  $N$  is the number of finite element nodes. For a more detailed description of all steps of the method we refer to [16]. The method has been further developed in [4] and [30] to also handle contact points and joining points.

## 2.4 Measures of variation

In general when variation simulation is done as part of the geometry assurance process, there are certain critical areas or points of the geometry where the resulting variation is measured. However, since we are testing and evaluating new variation simulation methodologies we are interested in how much variation we get in total for a part, subassembly or the complete assembly. Values will be compared between variation simulation procedures including composite specific features and the traditional methods. It is therefore reasonable to have a measure that gives one value for the total assembly. The root mean square (RMS) of the variance gives one such measure and the maximum displacement in the assembly gives another such a measure. These two measures will be derived and explained further in this section. We assume here that the assembly of interest consists of compliant parts with defined finite element (FE) meshes.

Since we assume a normal distribution for the input data and since we assume a linear response, the resulting output data will also be normally distributed. Hence we can compute the variance and the mean value for the output parameters, i.e., the displacement in each space direction  $(x, y, z)$  in each FE node. The sample variance in node  $i = 1, \dots, N$  in the direction  $\alpha = x, y, z$ , where  $N$  is the number of finite element mesh nodes, is given by

$$\sigma_{i\alpha}^2 = \frac{1}{M-1} \sum_{k=1}^M (t_{i\alpha k} - \bar{t}_{i\alpha})^2, \quad (2.3)$$

where  $t_{i\alpha k}$  is the displacement in direction  $\alpha$  in Monte Carlo iteration  $k$  for node  $i$ , and  $\bar{t}_{i\alpha}$  is the mean displacement in direction  $\alpha$  over all  $M$  Monte Carlo iterations for node  $i$ . A measure of total variation in each node is

$$\sigma_i^2 = \sigma_{ix}^2 + \sigma_{iy}^2 + \sigma_{iz}^2. \quad (2.4)$$

From this we can compute the RMS as a global measure of the total variation

$$\sigma_{\text{RMS}} = \sqrt{\frac{1}{N} \sum_{i=1}^N \sigma_i^2}. \quad (2.5)$$

If the variation in a certain direction,  $\alpha$ , is of specific interest we can use the global directional measure

$$\sigma_{\text{RMS}}^\alpha = \sqrt{\frac{1}{N} \sum_{i=1}^N \sigma_{i\alpha}^2}. \quad (2.6)$$

Since the quantity  $6\sigma$  is commonly used as the specification limit for acceptable geometric perturbation, we will use,  $6\sigma_{\text{RMS}}$  and  $6\sigma_{\text{RMS}}^\alpha$  as measures of total variation.

To capture possibly large local variation behavior in the assembly the maximum node variance can be used as a measure. It is calculated simply by taking the maximum over all nodes of the square root of (2.4), i.e.,

$$\sigma_{\max} = \max_{i \in \{1, \dots, N\}} \sigma_i = \max_{i \in \{1, \dots, N\}} \sqrt{\sigma_{ix}^2 + \sigma_{iy}^2 + \sigma_{iz}^2}. \quad (2.7)$$

# Chapter 3

## A brief introduction to composites

The aim with this section is to introduce terminology together with some basic knowledge about composite materials (Section 3.1) and the production processes used (Section 3.2). Further, some issues likely to affect the result of variation simulation will be discussed (Section 3.3). An extensive description of composites may be found in [3].

### 3.1 Materials

Composite materials are materials compound of two or more single materials with different engineering properties. The idea is that the composition of the materials should have different properties compared to the components themselves. In the finished composite the components are suitably arranged and still distinguishable. A simple generic example of a composite is concrete that is compound of rocks and clay. Though, when talking about the huge increase in use of composite materials in industries it is rather fibrous composites or laminated composites that are discussed.

Fibrous composites consists of a matrix of e.g. polymer, metal or ceramic, reinforced with fibers of e.g. glass, boron, carbon, organic or alumina. Further, there exist different lengths of fibers, short and long fibers. The short fibers are randomly oriented whereas the long fibers, i.e., continuous fibers, are structured

along one direction, see Figure 3.1. In the following, when fibrous composites are discussed, it is assumed to be long fibers. Another type of composites are granulated composites, i.e., the matrix reinforcement has the shape of spheres. However fibrous composites, have shown to be stronger and therefore much more frequently used. One of the most common such composite is carbon fiber reinforced polymer (CFRP) with epoxy as the matrix material.

Laminated composites are compound of two or more plies of e.g. fibrous or granulated composites. A laminate consisting of plies of fibrous composites with different fiber orientation are common. The ply itself is orthotropic with three symmetry planes. The laminate, with such plies, have properties closer to isotropic materials.

The benefit of using composite materials instead of traditional materials such as different metals is that they are highly customizable. Differences between composites and metals are, above all, seen in the engineering properties such as weight, thermal expansion, stiffness, strength and fatigue resistance. A great advantage of the composites, compared to metals, is the stiffness to weight ratio. Further, in composites, stiffness and strength can be prioritized and gained where needed.

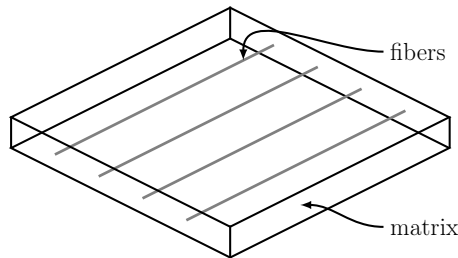


Figure 3.1: Fibrous composite with continuous fibers.

## 3.2 Production processes

Production of fibrous composites could, somewhat simplified, be divided into two categories. In the first category, fibers are placed first, either by hand layup or by automatic fiber placement, and then matrix resin is added. In the second category both fibers and resin are placed simultaneously either by automatic tape laying or by hand using prepregs, i.e. preimpregnated fibers.

After fibers and resin has been put into place the composite part need to be

cured for the matrix resin to harden. This can be done in room temperature but usually it is done in an autoclave, an oven, that could be pressurized. The temperature is often around  $80 - 150^\circ \text{C}$ , but could be as high as  $200^\circ \text{C}$ . Curing time is negatively proportional to the curing temperature.

For a complete description of the production processes available we refer to literature, see e.g. [9].

### 3.3 Uncertainties in composite production

The many different types of composites and their production processes suffer from various problems that may affect the geometric variation of an assembly. It could be hard to say beforehand how much the composite assembly variation is affected by these problems. One way to find out is to include them into the variation simulation. If the production process variations cause the mechanical properties of the composite part to change, the geometric variation will probably be affected.

Here we discuss the deviation from nominal ply thickness and the deviation in the fiber orientation (Section 3.3.1), that both are included in the model presented in Paper I, as well as the Spring-in phenomena (Section 3.3.2), that is captured in the model presented in Paper II.

#### 3.3.1 Ply thickness and fiber orientation

In laminate composite production the thickness of each ply is not exact. In fact the ply thicknesses can vary as much as 20% from specification [8]. Further, the process of putting together a laminae involve perturbations causing the fiber orientations to deviate from specification, [2]. These perturbations in ply thickness and fiber orientation can cause the mechanical properties of the composite product to change. Then the variation simulation will probably be inaccurate.

#### 3.3.2 Spring-in phenomena

During the curing process the composite part is kept in a fixture. Due to its anisotropic properties, such as the difference in coefficients of thermal expansion (CTE) between fibers and matrix as well as a chemical transition occurring only

in the matrix, stresses are built up when the part is cooled to room temperature. Hence, when released from the fixture these stresses cause a spring-back effect resulting in deformation of the part.

For certain types of geometries this spring-back effect is more significant than for others. In angled structures, such as T-beams and L-beams, the spring-back deformation cause a decrease of the angle between the flange and the web of the geometry, see Figure 3.2. In these special cases the effect is called spring-in. In Paper II we propose a method to include the process variation from curing by solving the FEM thermal expansion problem for the cooling after curing.



Figure 3.2: The spring-in phenomenon shown on an L-beam.

# Chapter 4

## FEM for composite shells

In this chapter we present the finite element method (FEM) used for solving the deformation of the composite parts. The main purpose of the chapter is to define concepts and terminology needed to understand the papers. In Paper I we include variations in the composite fiber directions as well as the ply thicknesses and in Paper II we solve a FEM thermal expansion problem. In this chapter we will state the equations describing the composite fiber directions, the ply thicknesses, as well as the thermal expansion. This should give an understanding to the process parameter variations performed in the papers.

Since we only consider small deformations in the calculations for the papers, we here present only the linear structural mechanics theory. First we give the analytic equations and derive the variational formulation and the finite element formulation for the solid elements (Section 4.1) including thermal expansion for these. Then we give a general idea on how shell element theory can be derived from reducing the solid element theory (Section 4.2). Finally, we state the composite material specific parts of the equations (Section 4.3).

### Terminology

There are some notational conventions used in this Chapter:

The summation convention	$u_i^h \mathbf{e}_i := \sum_{i=1}^{n_{dim}} u_i^h \mathbf{e}_i$
Derivative notation:	$u_{i,j} := \frac{\partial u_i}{x_j}$
Symmetric derivatives:	$u_{(i,j)} := \frac{1}{2}(u_{i,j} + u_{j,i})$
Indices:	latin indices, $i, j, k, l = 1, 2, 3$ and greek indices, $\alpha, \beta, \gamma, \lambda = 1, 2$

## 4.1 Solid elements

In this section we will introduce the concept of deformation, strain, stress and the constitutive relation between these. First, assume we have a body,  $\Omega$ , in  $d = 2$  or 3 dimensions with boundary  $\Gamma$ . Further we assume that there are two kind of forces acting on it; body forces,  $\mathbf{f}$  and surface forces,  $\mathbf{h}$ . Surface forces are considered both on the external surface  $\Gamma$  as well as on internal surfaces of sections of the body.

### Stress

The vector of surface forces,  $\mathbf{h}$ , often referred to as the traction vector, for a given point is related to a normal vector,  $\mathbf{n}$ , of the surface and a stress tensor,  $\boldsymbol{\sigma}$ , such that

$$\mathbf{h} = \boldsymbol{\sigma} \mathbf{n}, \quad (4.1)$$

where

$$\boldsymbol{\sigma} = \begin{bmatrix} \sigma_{11} & \sigma_{12} & \sigma_{13} \\ \sigma_{21} & \sigma_{22} & \sigma_{23} \\ \sigma_{31} & \sigma_{32} & \sigma_{33} \end{bmatrix} \quad (4.2)$$

A component  $\sigma_{ij}$  is the stress acting in the direction  $x_j$  on a surface with normal parallel to the  $x_i$  axis. The components  $\sigma_{11}$ ,  $\sigma_{22}$  and  $\sigma_{33}$  are called *normal stresses* whereas  $\sigma_{12}$ ,  $\sigma_{13}$ ,  $\sigma_{21}$ ,  $\sigma_{23}$ ,  $\sigma_{31}$  and  $\sigma_{32}$  are termed *shear stresses*. It can be shown that  $\boldsymbol{\sigma}$  is symmetric.

Within the body  $\Omega$ , we need to make sure equilibrium of forces are satisfied, i.e.

$$\int_{\Gamma} \boldsymbol{\sigma} \mathbf{n} \, d\Gamma + \int_{\Omega} \mathbf{f} \, d\Omega = \mathbf{0} \quad (4.3)$$

By Gauss' divergence theorem this can be reformulated to a single integral on  $\Omega$ . Then we get the equilibrium condition that is part of the differential equation problem stated later in this section.

### Strain

Next we consider the deformation of the body, the strain. A deformation is recognised by a change of distance between two neighbouring material points or a change of angle between two intersecting lines.

The strain is described by the strain tensor  $\boldsymbol{\epsilon}$  with components  $\epsilon_{ij}$ . Similar to the stresses, there are *normal strain* and *shear strain* components.

To derive the normal strain, take two points  $\mathbf{p}$  and  $\mathbf{q}$  infinitesimally close with coordinates  $(x_1, x_2, x_3)$  and  $(x_1 + dx_1, x_2 + dx_2, x_3 + dx_3)$ . Let  $\mathbf{u} = \mathbf{u}(x_1, x_2, x_3)$  be a displacement function. Let  $\mathbf{p}'$  and  $\mathbf{q}'$  be the points  $\mathbf{p}$  and  $\mathbf{q}$  after deformation, i.e.

$$\mathbf{p}' = \mathbf{u}(x_1, x_2, x_3) \quad (4.4)$$

$$\mathbf{q}' = \mathbf{u}(x_1, x_2, x_3) + d\mathbf{u}(x_1, x_2, x_3) \quad (4.5)$$

where the vector  $d\mathbf{u}(x_1, x_2, x_3)$  is defined as

$$d\mathbf{u} = \begin{bmatrix} u_{1,1}dx_1 + u_{1,2}dx_2 + u_{1,3}dx_3 \\ u_{2,1}dx_1 + u_{2,2}dx_2 + u_{2,3}dx_3 \\ u_{3,1}dx_1 + u_{3,2}dx_2 + u_{3,3}dx_3 \end{bmatrix} \quad (4.6)$$

Now let  $\overline{\mathbf{pq}}$  denote the line between  $\mathbf{p}$  and  $\mathbf{q}$  and  $\overline{\mathbf{p}'\mathbf{q}'}$  the line between  $\mathbf{p}'$  and  $\mathbf{q}'$ . First, assume that both  $\overline{\mathbf{pq}}$  and  $\overline{\mathbf{p}'\mathbf{q}'}$  are parallel to the  $x_1$ -axis, i.e.  $dx_2 = dx_3 = 0$ . We want to calculate the relative elongation of  $\overline{\mathbf{pq}}$  after deformation, i.e.

$$\frac{|\overline{\mathbf{p}'\mathbf{q}'}| - |\overline{\mathbf{pq}}|}{|\overline{\mathbf{pq}}|}. \quad (4.7)$$

We have

$$|\overline{\mathbf{pq}}| = dx_1 \quad (4.8)$$

$$\begin{aligned} |\overline{\mathbf{p}'\mathbf{q}'}| &= |\mathbf{u}(\mathbf{q}') - \mathbf{u}(\mathbf{p}')| \\ &= dx_1 \sqrt{(1 + u_{1,1})^2 + u_{2,1}^2 + u_{3,1}^2} \end{aligned} \quad (4.9)$$

Since we consider small deformations here we can assume that

$$|u_{1,1}| \ll 1, \quad |u_{2,1}| \ll 1, \quad |u_{3,1}| \ll 1, \quad (4.10)$$

so that

$$|\overline{\mathbf{p}'\mathbf{q}'}| = dx_1(1 + u_{1,1}). \quad (4.11)$$

Then the relative elongation is

$$\frac{|\overline{\mathbf{p}'\mathbf{q}'}| - |\overline{\mathbf{pq}}|}{|\overline{\mathbf{pq}}|} = \frac{1}{dx_1} (dx_1(1 + u_{1,1}) - dx_1) = u_{1,1}. \quad (4.12)$$

This is the normal strain in the  $x_1$ -direction denoted  $\epsilon_{11}$ . Analogously we get the normal strain in the directions of the  $x_2$ - and  $x_3$ -axis denoted  $\epsilon_{22}$  and  $\epsilon_{33}$ .

To derive the shear strain the angle between two intersecting lines should be considered. Again the small deformation assumption is used to get the shear strain components  $\epsilon_{12}$ ,  $\epsilon_{13}$  and  $\epsilon_{23}$ . For this derivation we refer to e.g. [24].

So, the strain components are given by

$$\epsilon_{ij} = \frac{1}{2}u_{(i,j)} := \frac{1}{2}(u_{i,j} + u_{j,i}) \quad (4.13)$$

The strain tensor  $\epsilon$  is symmetric.

### Constitutive relation

The constitutive relation is the relation between the stress and the strain and depends on the material properties. Examples of constitutive relations are elasticity, plasticity, viscoelasticity. The simplest relation is linear elasticity which in one dimension is exactly Hooke's law

$$\sigma = E\epsilon \quad (4.14)$$

where the elastic coefficient  $E$  is Young's modulus. Elasticity means that material response is history independent, i.e. there is a one-to-one relation between stress and strain. More generally this relation is described by

$$\sigma_{ij} = c_{ijkl}\epsilon_{kl}, \quad (4.15)$$

where  $c_{ijkl}$  are elastic coefficients assumed to satisfy symmetry:

$$c_{ijkl} = c_{klij} \quad [\text{major symmetry}] \quad (4.16a)$$

$$c_{ijkl} = c_{jikl} \quad [\text{minor symmetry}] \quad (4.16b)$$

$$c_{ijkl} = c_{ijlk} \quad [\text{minor symmetry}] \quad (4.16c)$$

and positive definiteness

$$c_{ijkl}(\mathbf{x})\psi_{ij}\psi_{kl} \geq 0 \quad (4.16d)$$

$$c_{ijkl}(\mathbf{x})\psi_{ij}\psi_{kl} = 0 \Rightarrow \psi_{ij} = 0 \quad (4.16e)$$

Having this relation we are now able to formulate *the deformation problem*, i.e., the differential equation problem:

Given  $f_i : \Omega \rightarrow \mathbb{R}$ ,  $g_i : \Gamma_{g_i} \rightarrow \mathbb{R}$ ,  $h_i : \Gamma_{h_i} \rightarrow \mathbb{R}$ , find  $u_i : \bar{\Omega} \rightarrow \mathbb{R}$  such that

$$\frac{\partial \sigma_{ij}}{\partial x_j} + f_i = 0, \quad \text{in } \Omega \quad (4.17a)$$

$$u_i = g_i, \quad \text{on } \Gamma_{g_i} \quad (4.17b)$$

$$\sigma_{ij} n_j = h_i, \quad \text{on } \Gamma_{h_i} \quad (4.17c)$$

where  $g_i$  is prescribed boundary displacement,  $h_i$  is traction and  $\Gamma_{g_i}$ ,  $\Gamma_{h_i}$  are boundary segments such that  $\overline{\Gamma_{g_i} \cup \Gamma_{h_i}} = \Gamma$  and  $\Gamma_{g_i} \cap \Gamma_{h_i} = \emptyset$ . The equation (4.17a) is called the *equilibrium condition*. The properties (4.16) will assure that the deformation problem (4.17) have a unique solution.

### Weak form

Multiply (4.17a) by the test function  $w_i$  and integrate over  $\Omega$ :

$$\underbrace{\int_{\Omega} w_i \sigma_{ij,j} d\Omega}_{I_1} + \int_{\Omega} w_i f_i d\Omega = 0. \quad (4.18)$$

For the first integral,  $I_1$ , using integration by parts and that  $w_i = 0$  on  $\gamma_{g_i}$  we get

$$\begin{aligned} I_1 &= - \int_{\Omega} w_{i,j} \sigma_{ij} d\Omega + \int_{\Gamma} w_i \sigma_{ij} n_j d\Gamma \\ &= - \int_{\Omega} w_{i,j} \sigma_{ij} d\Omega + \sum_{i=1}^d \int_{\Gamma_{h_i}} w_i \sigma_{ij} n_j d\Gamma_{h_i} \\ &= - \int_{\Omega} w_{i,j} \sigma_{ij} d\Omega + \sum_{i=1}^d \int_{\Gamma_{h_i}} w_i h_i d\Gamma_{h_i} \end{aligned} \quad (4.19)$$

Now, moving constants to the right hand side, the weak form is

$$\int_{\Omega} w_{i,j} \sigma_{ij} d\Omega = \int_{\Omega} w_i f_i d\Omega + \sum_{i=1}^d \int_{\Gamma_{h_i}} w_i h_i d\Gamma_{h_i} \quad (4.20)$$

We will further rewrite the left hand side slightly. To do this, observe that a general nonsymmetric tensor  $s_{ij}$  can be decomposed into a sum of a symmetric

tensor and a skew-symmetric tensor;

$$s_{(ij)} := \frac{1}{2}(s_{ij} + s_{ji}) \quad [\text{symmetric}] \quad (4.21)$$

$$s_{[ij]} := \frac{1}{2}(s_{ij} - s_{ji}) \quad [\text{skew-symmetric}] \quad (4.22)$$

so that

$$s_{ij} = s_{(ij)} + s_{[ij]}. \quad (4.23)$$

Then for a general non symmetric tensor  $s_{ij}$  and a general symmetric tensor  $t_{ij}$  we have

$$s_{ij}t_{ij} = s_{(ij)}t_{ij}. \quad (4.24)$$

To show this, first by (4.23)

$$s_{ij}t_{ij} = s_{(ij)}t_{ij} + s_{[ij]}t_{ij}. \quad (4.25)$$

Then

$$s_{[ij]}t_{ij} = -s_{[ji]}t_{ij} = -s_{[ji]}t_{ji} \quad (4.26)$$

which implies that  $s_{[ij]}t_{ij} = 0$  and hence gives the result.

Using the result (4.24) with  $s_{ij} = w_{i,j}$  and  $t_{ij} = \sigma_{ij}$  gives

$$w_{i,j}\sigma_{ij} = \frac{1}{2}(w_{i,j} + w_{j,i})\sigma_{ij} \quad (4.27)$$

so that (4.20) becomes

$$\int_{\Omega} w_{(i,j)}\sigma_{ij} \, d\Omega = \int_{\Omega} w_i f_i \, d\Omega + \sum_{i=1}^d \int_{\Gamma_{h_i}} w_i h_i \, d\Gamma_{h_i} \quad (4.28)$$

We introduce the abstract notation for this

$$a(\mathbf{w}, \mathbf{u}) = \int_{\Omega} w_{(i,j)} c_{ijkl} u_{(k,l)} \, d\Omega \quad (4.29a)$$

$$(\mathbf{w}, \mathbf{f}) = \int_{\Omega} w_i f_i \, d\Omega \quad (4.29b)$$

$$(\mathbf{w}, \mathbf{h})_{\Gamma} = \sum_{i=1}^d \left( \int_{\Gamma_{h_i}} w_i h_i \, d\Gamma \right) \quad (4.29c)$$

Define the trial space  $\mathcal{S} = \{\mathbf{u} \in H^1(\Omega)^d; u_i = g_i \text{ on } \Gamma_{g_i}\}$  and the test space  $\mathcal{V} = \{\mathbf{w} \in H^1(\Omega)^d; w_i = 0 \text{ on } \Gamma_{g_i}\}$ . Further to simplify notation let  $\Gamma_{\mathbf{g}} =$

$\Gamma_{g_1} \times \cdots \times \Gamma_{g_d}$  and  $\Gamma_{\mathbf{h}} = \Gamma_{h_1} \times \cdots \times \Gamma_{h_d}$ . Then the deformation problem in weak form is:

Given  $\mathbf{f} \in L_2(\Omega)^d : \Omega \rightarrow \mathbb{R}^d$ ,  $\mathbf{g} \in L_2(\Gamma_{\mathbf{g}})^d : \Gamma_{\mathbf{g}} \rightarrow \mathbb{R}^d$  and  $\mathbf{h} \in L_2(\Gamma_{\mathbf{h}})^d : \Gamma_{\mathbf{h}} \rightarrow \mathbb{R}^d$ , find  $\mathbf{u} \in \mathcal{S}$  such that for all  $\mathbf{w} \in \mathcal{V}$

$$a(\mathbf{w}, \mathbf{u}) = (\mathbf{w}, \mathbf{f}) + (\mathbf{w}, \mathbf{h})_{\Gamma} \quad (4.30)$$

### Discrete form

Now to take the step to a FEM-formulation we first assume a triangulation of the domain  $\Omega$ . Based on this finite element representation we define the discrete spaces  $\mathcal{S}^h = \{\mathbf{u}^h \in H^1(\Omega)^d; \mathbf{u}^h \text{ continuous piecewise linear with } u_i^h = g_i^h \text{ on } \Gamma_{g_i}\}$  and  $\mathcal{V}^h = \{\mathbf{w}^h \in H^1(\Omega)^d; \mathbf{w}^h \text{ continuous piecewise linear with } w_i^h = 0 \text{ on } \Gamma_{g_i}\}$ . Further we will consider the decomposition

$$\mathbf{u}^h = \mathbf{v}^h + \mathbf{g}^h,$$

where  $\mathbf{v}^h \in \mathcal{V}^h$  and  $\mathbf{g}^h$  is the (known) prescribed boundary displacement. The FEM problem then reads;

Given  $\mathbf{f} \in L_2(\Omega)^d : \Omega \rightarrow \mathbb{R}^d$ ,  $\mathbf{g} \in L_2(\Gamma_{\mathbf{g}})^d : \Gamma_{\mathbf{g}} \rightarrow \mathbb{R}^d$  and  $\mathbf{h} \in L_2(\Gamma_{\mathbf{h}})^d : \Gamma_{\mathbf{h}} \rightarrow \mathbb{R}^d$ , find  $\mathbf{v}^h \in \mathcal{V}^h$  such that for all  $\mathbf{w}^h \in \mathcal{V}^h$

$$a(\mathbf{w}^h, \mathbf{v}^h) = (\mathbf{w}^h, \mathbf{f}) + (\mathbf{w}^h, \mathbf{h})_{\Gamma} - a(\mathbf{w}^h, \mathbf{g}^h) \quad (4.31)$$

$$\mathbf{u}^h = \mathbf{v}^h + \mathbf{g}^h \quad (4.32)$$

### Matrix-vector form

Next we want to write (4.31) on matrix form. Let  $N^A$  denote the shape functions corresponding to the triangulation of  $\Omega$  where  $A \in I = \{1, 2, \dots, n\}$ , where  $n$  is the number of nodes in the triangulation. Define also the index set  $I_{g_i} = \{A \in I; u_i^h = g_i\}$ , i.e. the set of nodes at which a dirichlet boundary condition in the direction  $i = 1, \dots, d$  is present.

Now with the shape functions we can write

$$v_i^h = \sum_{A \in I \setminus I_{g_i}} N^A d_i^A \quad (4.33a)$$

$$g_i^h = \sum_{A \in I_{g_i}} N^A g_i^A \quad (4.33b)$$

where  $d_i^A, g_i^A \in \mathbb{R}$  and  $g_i^A$  is the right hand side function of the dirichlet boundary condition (4.17b) evaluated at  $x_i^A$ . Further letting  $\mathbf{e}_i$  denote basis vectors in  $\mathbb{R}^d$  we have

$$\mathbf{v}^h = v_i^h \mathbf{e}_i \quad (4.34a)$$

$$\mathbf{g}^h = g_i^h \mathbf{e}_i \quad (4.34b)$$

For a fix  $i$ , use the shape functions as test function, i.e.

$$\mathbf{w}^h = N^A \mathbf{e}_i, \quad A \in I \setminus I_{g_i} \quad (4.35)$$

and substitute (4.34) into (4.31) which gives

$$\begin{aligned} a\left(N^A \mathbf{e}_i, \sum_{B \in I \setminus I_{g_j}} N^B d_j^B \mathbf{e}_j\right) \\ = \left(N^A \mathbf{e}_i, \mathbf{f}\right) + \left(N^A \mathbf{e}_i, \mathbf{h}\right)_\Gamma - a\left(N^A \mathbf{e}_i, \sum_{B \in I_{g_j}} N^B g_j^B \mathbf{e}_j\right) \end{aligned} \quad (4.36)$$

And from bilinearity of  $a(\cdot, \cdot)$  we get further

$$\begin{aligned} \sum_{B \in I \setminus I_{g_j}} a(N^A \mathbf{e}_i, N^B \mathbf{e}_j) d_j^B \\ = (N^A \mathbf{e}_i, \mathbf{f}) + (N^A \mathbf{e}_i, \mathbf{h})_\Gamma - \sum_{B \in I_{g_j}} a(N^A \mathbf{e}_i, N^B \mathbf{e}_j) g_j^B \end{aligned} \quad (4.37)$$

This should hold for all  $A \in I \setminus I_{g_i}$  and  $i = 1, \dots, d$ . Therefore we get a system of equations

$$\mathbf{Kd} = \mathbf{f}. \quad (4.38)$$

The number of equations in this system is

$$n_{\text{eq}} = \sum_{i=1}^d |I \setminus I_{g_i}|. \quad (4.39)$$

The stiffness matrix  $\mathbf{K}$  consists of  $d$ -by- $d$  blocks  $\mathbf{K}_{AB}$  for each node pair  $AB$  without boundary condition in any direction. If a boundary condition exist

in either node  $A$  or  $B$  or both in some direction the block is correspondingly smaller. The row and column corresponding to a boundary condition could instead be found in the right hand side. A general block looks like

$$\mathbf{K}_{AB} = a(N^A \mathbf{e}_m, N^B \mathbf{e}_n) = \int_{\Omega} (N^A \mathbf{e}_m)_{(i,j)} c_{ijkl} (N^B \mathbf{e}_n)_{(k,l)} d\Omega, \quad (4.40)$$

for  $m, n = 1, \dots, d$ , where  $A \in I \setminus I_{g_m}$  and  $B \in I \setminus I_{g_n}$ . The vector  $\mathbf{f}$  is built up of corresponding  $d$ -by-1 pieces (or smaller if a boundary condition is present)

$$\begin{aligned} \mathbf{f}_A &= (N^A \mathbf{e}_m, \mathbf{f}) + (N^A \mathbf{e}_m, \mathbf{h})_{\Gamma} - \sum_{B \in I_{g_n}} a(N^A \mathbf{e}_m, N^B \mathbf{e}_n) g_n^B \\ &= \int_{\Omega} N^A f_m d\Omega + \int_{\Gamma_{h_m}} N^A h_m d\Gamma \\ &\quad - \sum_{B \in I_{g_n}} \left( \int_{\Omega} (N^A \mathbf{e}_m)_{(i,j)} c_{ijkl} (N^B \mathbf{e}_n)_{(k,l)} d\Omega \right) g_n^B, \end{aligned} \quad (4.41)$$

for  $m = 1, \dots, d$ . Similarly for the solution vector  $\mathbf{d}$

$$\mathbf{d}_B = d_n^B, \quad n = 1, \dots, d \quad (4.42)$$

For an isotropic body the elastic coefficients  $c_{ijkl}$  are

$$c_{ijkl}(x) = \mu(x)(\delta_{ik}\delta_{jl} + \delta_{il}\delta_{jk}) + \lambda(x)\delta_{ij}\delta_{kl} \quad (4.43)$$

where  $\lambda$  and  $\mu$  are Lamé parameters related to the engineering constants  $E$ , Young's modulus, and  $\nu$ , Poisson's ratio, such that

$$\mu = \frac{E}{2(1+\nu)}, \quad \lambda = \frac{\nu E}{(1+\nu)(1-2\nu)} \quad (4.44)$$

In the isotropic case then

$$\mathbf{K}_{AB} = \int_{\Omega} \left( \mu(\nabla N^B \otimes \nabla N^A + \nabla N^A \cdot \nabla N^B \mathbf{I}) + \lambda \nabla N^A \otimes \nabla N^B \right) d\Omega \quad (4.45)$$

where  $\otimes$  and  $\cdot$  is the outer product and scalar product respectively,  $\mathbf{I}$  is the identity matrix and  $\nabla N^A = [N_{,1}^A, \dots, N_{,d}^A]^{\top}$ .

## 4.2 Shell model

There are many approaches to reach a linear finite element shell formulation, see e.g. [24, 13]. Here we will derive a linear shell formulation by reduction of

the solid elements into shell elements with the middle surface as a reference surface, see [11]. With this approach the geometry for the shell mesh can be described by

$$\mathbf{x}(\xi, \eta, \zeta) = \mathbf{X}(\xi, \eta) + \bar{\mathbf{x}}(\xi, \eta, \zeta) \quad (4.46)$$

where  $\xi, \eta, \zeta \in [0, 1]$ ,  $\mathbf{x} \in \mathbb{R}^3$  is arbitrary point in the shell,  $\mathbf{X}$  is a point in the reference surface and  $\bar{\mathbf{x}}$  is a direction vector, referred to as the *director*, from  $\mathbf{X}$  to  $\mathbf{x}$ .

To be able to formulate the FEM equations for the shell we will need two types of local coordinate systems defined relative to the shell element. First the *lamina coordinate system*, which is defined in each integration point (i.e., the element points used for the numerical integration). Second, *the director coordinate system*, which is defined in each FE node. For the exact definition and how to compute these bases we refer to [11].

The lamina coordinate system with basis vectors  $\mathbf{e}_1^l, \mathbf{e}_2^l, \mathbf{e}_3^l$ , is created such that  $\mathbf{e}_3^l$  is the unit normal to the lamina. The two other basis vectors,  $\mathbf{e}_1^l$  and  $\mathbf{e}_2^l$ , are defined such that they are as close to the gradient vectors  $\mathbf{X}_{,\xi}$  and  $\mathbf{X}_{,\eta}$  as possible respectively in some sense.

The basis for the director coordinate system,  $\mathbf{e}_1^A, \mathbf{e}_2^A, \mathbf{e}_3^A$ , is defined such that  $\mathbf{e}_3^A$  is tangent to the director. Then  $\mathbf{e}_1^A$  and  $\mathbf{e}_2^A$  are defined as close to the global coordinate basis vectors  $\mathbf{e}_1$  and  $\mathbf{e}_2$  as possible respectively in some sense.

The displacements of the shell element is described by the kinematic equations formulated in the global coordinate system

$$\mathbf{u}(\xi, \eta, \zeta) = \mathbf{U}(\xi, \eta) + \bar{\mathbf{u}}(\xi, \eta, \zeta) \quad (4.47)$$

where  $\mathbf{u} \in \mathbb{R}^3$  is displacement of arbitrary point in the shell,  $\mathbf{U}$  is displacement of a point on the middle surface and  $\bar{\mathbf{u}}$  is displacement of the director. The finite element discretization of  $\mathbf{u}(\xi, \eta, \zeta)$  and the test function  $\mathbf{w}(\xi, \eta, \zeta)$  is formulated as

$$\mathbf{u}(\xi, \eta, \zeta) = \sum_{A=1}^{n_{en}} N^A \mathbf{U}^A + z^A(\zeta) N^A (\theta_2^A \mathbf{e}_1^A - \theta_1^A \mathbf{e}_2^A) \quad (4.48)$$

$$\mathbf{w}(\xi, \eta, \zeta) = \sum_{A=1}^{n_{en}} N^A \mathbf{w}^A + z^A(\zeta) N^A (\varphi_2^A \mathbf{e}_1^A - \varphi_1^A \mathbf{e}_2^A) \quad (4.49)$$

where  $N^A = N^A(\xi, \eta)$  is the shape function for node A,  $\mathbf{U}^A$  and  $\mathbf{w}^A$  are nodal coefficients,  $z^A$  is a thickness function,  $\theta_1^A$  and  $\theta_2^A$ , with test functions  $\varphi_1^A$  and  $\varphi_2^A$  respectively, are rotation of the director about the  $\mathbf{e}_1^A$  and  $\mathbf{e}_2^A$  respectively.

By this discretization of  $\mathbf{u}$  we have assumed that displacements are constant through the thickness, i.e., the directors can not stretch.

To derive the finite element shell formulation we start with the variational equation for the solid elements, (4.28), and for simplicity we assume no Neumann boundary condition. So we start with

$$\int_{\Omega} w_{(i,j)} \sigma_{ij} \, d\Omega = \int_{\Omega} w_i f_i \, d\Omega \quad (4.50)$$

and replace the volume integral  $\int_{\Omega} \cdot \, d\Omega$  by an integral over the shell thickness inside an integral over the shell elements in lamina coordinates, i.e.,  $\int_S \int_{-1}^1 \cdot \, d\zeta \, d\xi \, d\eta$ , where  $S$  is the two-dimensional unit square. For all variables written in lamina coordinates, the superscript  $l$  is used for convenience. Further, we assume *the zero normal stress condition* holds. This means that the stress component along the lamina 3-direction,  $\sigma_{33}^l$  is set to be zero. This assumption implies that we can derive an expression for the strain component  $\epsilon_{33}^l$  and eliminate it. Hence, the constitutive equation is given by

$$\sigma_{\alpha\beta}^l = c_{\alpha\beta\gamma\lambda}^l(\zeta) \epsilon_{\gamma\lambda}^l = c_{\alpha\beta\gamma\lambda}^l \left( \frac{1}{2} (u_{\gamma,\lambda}^l + u_{\lambda,\gamma}^l) \right) \quad (4.51)$$

$$\sigma_{\alpha 3}^l = c_{\alpha\beta}^l(\zeta) \epsilon_{\beta 3}^l = c_{\alpha\beta}^l (u_{3,\beta} + u_{\beta,3}) \quad (4.52)$$

Now with this assumption the shell equivalent of (4.50) is

$$\int_S \int_{-1}^1 \left( \underbrace{w_{(\alpha,\beta)}^l \sigma_{\alpha\beta}^l}_{I_1} + \underbrace{2w_{(\alpha,3)}^l \sigma_{\alpha 3}^l}_{I_2} \right) \det(\mathbf{J}_{\mathbf{x}}) \, d\zeta \, dS = \int_S \int_{-1}^1 w_i^l f_i^l \det(\mathbf{J}_{\mathbf{x}}) \, d\zeta \, dS \quad (4.53)$$

where  $\mathbf{J}_{\mathbf{x}} = \mathbf{J}(\mathbf{X}(\xi, \eta))$  is the jacobi matrix of the position vector  $\mathbf{x}$ . To expand the terms  $I_1$  and  $I_2$  further we need the derivative of  $\mathbf{u}^l$  with respect to lamina directions

$$u_{i,j}^l = \sum_{m=1}^3 e_{im}^l \sum_{A=1}^{n_{en}} (N_{,j}^A U_m^A + (z^A N^A)_{,j} (\theta_2^A e_{1m}^A - \theta_1^A e_{2m}^A)) \quad (4.54)$$

The symmetry of  $\sigma_{\alpha\beta}$  gives that  $w_{(\alpha,\beta)} \sigma_{\alpha\beta} = w_{\alpha,\beta} \sigma_{\alpha\beta}$ . Hence, for the first

integral term,  $I_1$ , we have

$$\begin{aligned}
\pi_1^A &= \int_S \int_{-1}^1 w_{\alpha,\beta}^{Al} \sigma_{\alpha\beta}^l \det(\mathbf{J}_\mathbf{x}) \, d\zeta dS \\
&= \int_S \int_{-1}^1 w_{\alpha,\beta}^{Al} c_{\alpha\beta\gamma\lambda}^l \epsilon_{\gamma\lambda}^l \det(\mathbf{J}_\mathbf{x}) \, d\zeta dS \\
&= \int_S \int_{-1}^1 [w_i^A e_{\alpha i}^l N_{,\beta}^A + (z^A N^A)_{,\beta} e_{\alpha i}^l (\varphi_2^A e_{1i}^A - \varphi_1^A e_{2i}^A)] c_{\alpha\beta\gamma\lambda}^l \\
&\quad [e_{\gamma j}^l N_{,\lambda}^B U_j^B + (N^B z^B)_{,\lambda} e_{\gamma j}^l (\theta_2^B e_{1j}^B - \theta_1^B e_{2j}^B)] \det(\mathbf{J}_\mathbf{x}) \, d\zeta dS \quad (4.55)
\end{aligned}$$

For the second term,  $I_2$ , we have

$$\begin{aligned}
\pi_2^A &= \int_S \int_{-1}^1 2w_{(\alpha,3)} \sigma_{\alpha 3} \det(\mathbf{J}_\mathbf{x}) \, d\zeta dS \\
&= \int_S \int_{-1}^1 2w_{(\alpha,3)} c_{\alpha\beta}^l \epsilon_{\beta 3}^l \det(\mathbf{J}_\mathbf{x}) \, d\zeta dS \\
&= \int_S \int_{-1}^1 \left[ e_{\alpha i}^l N^A (\varphi_3^A e_{1i}^A - \varphi_1^A e_{2i}^A) \right. \\
&\quad \left. + e_{3i}^l (N_{,\alpha}^A w_i^A + (z^A N^A)_{,\alpha} (\varphi_3^A e_{1i}^A - \varphi_1^A e_{2i}^A)) \right] c_{\alpha\beta}^l \\
&\quad \left[ \left( e_{\beta j}^l N^B (\theta_2^B e_{1j}^B - \theta_1^B e_{2j}^B) \right) \right. \\
&\quad \left. + e_{3j}^l (N_{,\beta}^B U_j^B + (z^B N^B)_{,\beta} (\theta_2^B e_{1j}^B - \theta_1^B e_{2j}^B)) \right] \det(\mathbf{J}_\mathbf{x}) \, d\zeta dS \quad (4.56)
\end{aligned}$$

Now we have reached the FEM formulation for the left hand side of the shell formulation (4.53).

$$\pi_1^A + \pi_2^A = \int_S \int_{-1}^1 w_i^l f_i^l \det(\mathbf{J}_\mathbf{x}) \, d\zeta dS \quad (4.57)$$

Since the composite material definitions, that we are interested in looking closer at, are contained in this part, we will not derive the FEM formulation for the right hand side, it can be found in e.g. [11].

We will make further assumptions which reduces the complexity of the expressions and allows an analytic integration through the thickness. Namely, assume that we have constant thickness, flat elements and three rotational dof (i.e., six

dof in total). Then we will arrive at

$$\begin{aligned} \pi_1^A = & \underbrace{\int_S w_i^A e_{\alpha i}^l N_{,\beta}^a c_{\alpha\beta\gamma\delta}^n e_{\gamma j}^l N_{,\delta}^B U_j^B \mathbf{J} \, dS}_{\text{membrane part}} \\ & + \underbrace{\int_S \varphi_i^A A_{\alpha i}^l N_{,\beta}^A c_{\alpha\beta\gamma\delta}^m N_{,\delta} A_{\gamma j}^l \theta_j^B \mathbf{J} \, dS}_{\text{bending part}} \end{aligned} \quad (4.58)$$

$$\pi_2^A = \int_S (w_i^A N_{,\alpha}^A e_{3i}^l + \varphi_i^A N^A A_{\alpha i}^l) c_{\alpha\beta}^s (e_{3j}^l N_{,\beta}^B U_j^B + N^B A_{\beta j}^l \theta_j^B) \mathbf{J} \, dS \quad (4.59)$$

where we have defined ( $\times$  denotes the cross product)

$$A_{\alpha i}^l = \mathbf{e}_\alpha^l \times \mathbf{e}_3^l \quad (4.60)$$

and

$$c_{\alpha\beta\gamma\delta}^n = \int_{-1}^1 c_{\alpha\beta\gamma\delta}^l(\zeta) \, d\zeta \quad (4.61a)$$

$$c_{\alpha\beta\gamma\delta}^m = \int_{-1}^1 c_{\alpha\beta\gamma\delta}^l(\zeta) z^2(\zeta) \, d\zeta \quad (4.61b)$$

$$c_{\alpha\beta}^s = \int_{-1}^1 c_{\alpha\beta}^l(\zeta) \, d\zeta \quad (4.61c)$$

which are computed before the assembly of the stiffness matrix starts. It is in the definition of the elastic coefficients, (4.61), we see what kind of material we have.

## 4.3 Composite shells

In this section we will show how the compliance matrix (or the inverse of it) is defined, i.e., how the elastic coefficients (4.61) are defined for composites.

### 4.3.1 Orthotropic material models

An orthotropic material is an anisotropic material which has three orthogonal symmetry planes. In this section we will see what the constitutive relation look like for an orthotropic material. That is, we will look at the definition of the elastic coefficients  $c_{\alpha\beta\gamma\delta}$ .

To simplify notation, we will use the voigt notation, i.e., the stress and strain tensors will be written on vector form. With the zero normal stress condition we define

$$\bar{\sigma} = \begin{bmatrix} \sigma_{11} \\ \sigma_{22} \\ \sigma_{12} \\ \sigma_{13} \\ \sigma_{23} \end{bmatrix}, \quad \bar{\epsilon} = \begin{bmatrix} \epsilon_{11} \\ \epsilon_{22} \\ 2\epsilon_{12} \\ 2\epsilon_{13} \\ 2\epsilon_{23} \end{bmatrix} \quad (4.62)$$

The coefficients of elasticity for orthotropic materials including plane stress written on voigt notation is, first for the part corresponding to  $c_{\alpha\beta\gamma\lambda}$

$$\mathbf{D}_1 = \begin{bmatrix} D_{11} & D_{12} & 0 \\ D_{12} & D_{22} & 0 \\ 0 & 0 & D_{66} \end{bmatrix} = \begin{bmatrix} c_{1111} & c_{1122} & 0 \\ c_{1122} & c_{2222} & 0 \\ 0 & 0 & c_{1212} \end{bmatrix} \quad (4.63)$$

and for the part corresponding to  $c_{\alpha\beta}$  it is

$$\mathbf{D}_2 = \begin{bmatrix} D_{44} & 0 \\ 0 & D_{55} \end{bmatrix} = \begin{bmatrix} c_{11} & 0 \\ 0 & c_{22} \end{bmatrix} \quad (4.64)$$

The complete matrix  $\mathbf{D}$  is

$$\mathbf{D} = \begin{bmatrix} D_{11} & D_{12} & 0 & 0 & 0 \\ D_{12} & D_{22} & 0 & 0 & 0 \\ 0 & 0 & D_{44} & 0 & 0 \\ 0 & 0 & 0 & D_{55} & 0 \\ 0 & 0 & 0 & 0 & D_{66} \end{bmatrix} \quad (4.65)$$

So the constitutive equation is

$$\bar{\sigma} = \mathbf{D}\bar{\epsilon} \quad (4.66)$$

The elements of the matrix  $\mathbf{D}$  are related to the six engineering constants:  $E_1$ ,  $E_2$ , the Young's modulus along the material axes 1 and 2,  $\nu_{12}$ , Poisson's ratio being the contraction in direction 2 when extended in direction 1, and  $G_{12}$ ,  $G_{13}$ ,  $G_{23}$ , the shear modulus in direction  $j$  (for  $G_{ij}$ ) on the plane with normal in direction  $i$ . So,

$$\begin{aligned} D_{11} &= \frac{E_1}{1-\nu_{12}\nu_{21}}, & D_{12} &= \frac{\nu_{12}E_2}{1-\nu_{12}\nu_{21}}, & D_{22} &= \frac{E_2}{1-\nu_{12}\nu_{21}} \\ D_{44} &= G_{23}, & D_{55} &= G_{13}, & D_{66} &= G_{12} \end{aligned} \quad (4.67)$$

where  $\frac{\nu_{12}}{E_1} = \frac{\nu_{21}}{E_2}$ , i.e.,  $\nu_{21} = \frac{E_2}{E_1}\nu_{12}$ .

Including also thermal expansion we have

$$\begin{bmatrix} \sigma_{11} \\ \sigma_{22} \\ \sigma_{12} \\ \sigma_{13} \\ \sigma_{23} \end{bmatrix} = \begin{bmatrix} \frac{E_1}{1-\nu_{12}\nu_{21}} & \frac{\nu_{12}E_2}{1-\nu_{12}\nu_{21}} & 0 & 0 & 0 \\ \frac{\nu_{12}E_2}{1-\nu_{12}\nu_{21}} & \frac{E_2}{1-\nu_{12}\nu_{21}} & 0 & 0 & 0 \\ 0 & 0 & G_{23} & 0 & 0 \\ 0 & 0 & 0 & G_{13} & 0 \\ 0 & 0 & 0 & 0 & G_{12} \end{bmatrix} \begin{bmatrix} \epsilon_{11} - \alpha_1 \Delta T \\ \epsilon_{22} - \alpha_2 \Delta T \\ 2\epsilon_{12} \\ 2\epsilon_{13} \\ 2\epsilon_{23} \end{bmatrix} \quad (4.68)$$

where  $\Delta T$  is the change in temperature and  $\alpha_1, \alpha_2$  are CTE.

Computing the inverse of  $\mathbf{D}$ , often called the compliance matrix  $\mathbf{C} = \mathbf{D}^{-1}$  gives

$$\begin{bmatrix} \epsilon_{11} - \alpha_1 \Delta T \\ \epsilon_{22} - \alpha_2 \Delta T \\ 2\epsilon_{12} \\ 2\epsilon_{13} \\ 2\epsilon_{23} \end{bmatrix} = \begin{bmatrix} \frac{1}{E_1} & -\frac{\nu_{21}}{E_2} & 0 & 0 & 0 \\ -\frac{\nu_{12}}{E_1} & \frac{1}{E_2} & 0 & 0 & 0 \\ 0 & 0 & \frac{1}{G_{23}} & 0 & 0 \\ 0 & 0 & 0 & \frac{1}{G_{13}} & 0 \\ 0 & 0 & 0 & 0 & \frac{1}{G_{12}} \end{bmatrix} \begin{bmatrix} \sigma_{11} \\ \sigma_{22} \\ \sigma_{12} \\ \sigma_{13} \\ \sigma_{23} \end{bmatrix} \quad (4.69)$$

The definition of the matrix  $\mathbf{D}$  here is written in material coordinates, i.e., the axis of symmetry. If we think of a fibrous composite the 1-direction would correspond to the fiber orientation. A transformation matrix  $\mathbf{T}$  can be applied to transform  $\mathbf{D}$  into lamina coordinates as needed in (4.61). The transformation matrix is defined as, see e.g. [11],

$$\mathbf{T} = \begin{bmatrix} \cos^2 \theta & \sin^2 \theta & 0 & 0 & 0 & -\sin 2\theta \\ \sin^2 \theta & \cos^2 \theta & 0 & 0 & 0 & \sin 2\theta \\ 0 & 0 & 1 & 0 & 0 & 0 \\ 0 & 0 & 0 & \cos \theta & \sin \theta & 0 \\ 0 & 0 & 0 & -\sin \theta & \cos \theta & 0 \\ \sin \theta \cos \theta & -\sin \theta \cos \theta & 0 & 0 & 0 & \cos^2 \theta - \sin^2 \theta \end{bmatrix} \quad (4.70)$$

where  $\theta$  is the angle representing the rotational difference between the material and the lamina coordinate systems. Then we can compute

$$\mathbf{D}^l = \mathbf{T} \mathbf{D} \mathbf{T}^\top \quad (4.71)$$

Finally, this matrix  $\mathbf{D}^l$  is used to compute the elastic coefficients (4.61).

Here we have derived the orthotropic material model for shells, but also solids could have orthotropic material. The derivations is similar, but there are six stress and strain components. With six strain components we also get a third CTE.

### 4.3.2 Laminae of orthotropic materials

To define a laminate of orthotropic plies, each ply is specified by setting the ply thickness and the fiber orientation. The fiber orientation is specified by an angle relating the material coordinates to the lamina coordinate system. For a laminate consisting of a number of plies with specified thickness and fiber orientation, we need to compute the matrix  $\mathbf{D}^l$  for each ply. Then in the integrals for the elastic coefficients (4.61),  $c_{\alpha\beta\gamma\lambda}(\zeta)$  and  $c_{\alpha\beta}(\zeta)$  are piecewise constants.

# Chapter 5

## Summary of papers

The variation simulations performed in the papers is the Monte Carlo based method implemented in the software RD&T [25].

In both papers, to discretize the part geometries, a finite element shell mesh is used. For the composite parts, layered shell meshes are used. The mesh consists mainly of quadrilateral elements but also of some triangular elements. As an intermediate step in the method presented in Paper II, the shell mesh is expanded into a solid mesh consisting of hexahedral elements together with some wedge elements.

For the FEM simulations carried out, the implementation in the software LaStFEM is used, [15]. This implementation is based on the shell formulation stated in [26, 12, 14, 13]. For other applications see also [20, 19, 18, 21, 23, 28].

A summary, with focus on describing the methods used in the two papers, is given here, (Paper I in Section 5.1 and Paper II in Section 5.2).

### **5.1 Paper I: Variation simulation for composite parts and assemblies including variation in fiber orientation and thickness**

In Paper I, a new method for performing variation simulation with composite parts is presented. In this method traditional variation simulation is extended

with variation simulation for uncertainties in ply thicknesses and fiber orientations. A summary of the method is given first (Section 5.1.1), then the testcase used to demonstrate the method (Section 5.1.2) and the results (Section 5.1.3) are presented in summary.

### 5.1.1 Method

In the method proposed in Paper I, variation simulation is carried out in two levels, the traditional variation simulation and the new part with variation in ply thickness and fiber orientation.

The input parameters in the model are divided into two groups:

- Material parameters
  - Fiber orientation.
  - Ply thickness.
- Geometric parameters
  - Locators.
  - Joining points.
  - Contact points.

First, we have studied what happens when the material parameters are at their extreme values (= LSL, USL). This is not likely to happen in practice, but theoretically it is interesting to see how this extreme setting affect the geometric variation. For each setting of the material parameters, a traditional variation simulation is performed where the geometric parameters with specified tolerances are the input, see Figure 5.1.



Figure 5.1: Variation simulation in two levels.

Second, we have performed variation simulation for the material parameters, i.e., the input setting is chosen by the MC method. Again for each material parameter setting a traditional variation simulation for the geometric parameters is performed.

The reason for the variation simulation in two levels is to see how the material parameter variation affects the traditional variation simulation. Keeping the variation simulations separate makes it easier to do this analysis.

### 5.1.2 Test case

The test case used to demonstrate the proposed method in the Paper is a subassembly from automotive industry consisting of two composite parts, see Figure 5.2. The parts are referred to as the *lower part* and the *upper part* as stated in Figure 5.2. Both parts are assumed to be laminae of fibrous composites, including 8 plies for the lower part and 6 plies for the upper part. It is assumed that the nominal thickness of each ply is equal, 2mm. The nominal fiber orientation of each ply is shown in Figure 5.3.

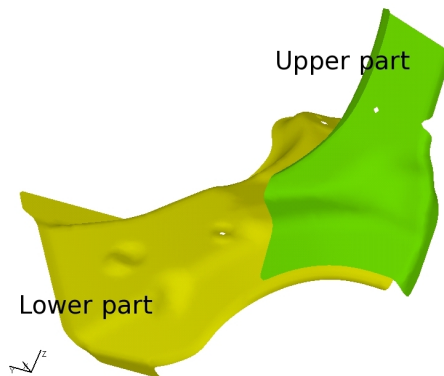


Figure 5.2: The subassembly used as test case in Paper I.

The number of input parameters for this test case is 28, each ply has one representing fiber orientation and one representing the ply thickness. The tolerances for the input parameters are stated in Table 5.1.

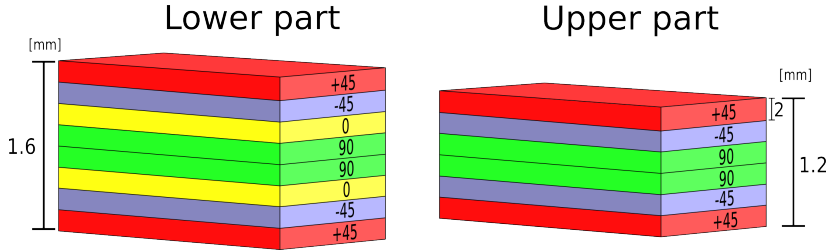


Figure 5.3: The composition of plies for the two composite parts in the test case showing the fiber orientation of the respective plies.

	description	tolerance, (LSL,USL at $\pm 4\sigma$ )
Material parameters	Fiber orientation	$\pm 13^\circ$
	Ply thickness	$\pm 20\%$
Geometric parameters	Locators	$\pm 0.1\text{mm}$
	Joining points	$\pm 0.1\text{mm}^*$

Table 5.1: Input parameters and tolerances. \*Relative individual tolerance, there is also a total tolerance for the group of joining points.

### 5.1.3 Results

The results presented in the paper, indicate that the inclusion of variation in the fiber orientations and ply thicknesses affect the standard variation simulations in such a way that the variance of the output distributions is approximately 10% larger. However, the results show no structural changes in the output distribution. Hence, according to these results, it is sufficient to use a correction factor to the traditional variation simulation results.

## 5.2 Paper II: Geometry assurance integrating process variation with simulation of spring-in for composite parts and assemblies

In Paper II we present a method where process variations from the composite curing process are captured. This method is then combined with the traditional variation simulations.

### 5.2.1 Method

To simulate the curing process we set an initial temperature, common to all parts in the assembly, and simulate the cooling by solving a FEM thermal expansion problem for each part. If the assembly consists of both metal and composite parts, which is possible, this is of course only done for the composites. The shrinkage occurring when the part is cooled to room temperature cause the composite part to deviate from nominal geometry. The thermal expansion simulation is done as a prestep to the traditional variation simulation, i.e., the initial geometry is deformed.

The input parameters we included in the model are:

- Process parameters
  - Curing temperature.
- Geometric parameters
  - Locators.
  - Joining points.
  - Contact points.

The displacement due to the thermal shrinkage is linearly dependent on the initial temperature. Hence, the process parameter for the temperature can be included in the precalculation of a solution basis according to the MIC method.

For the thermal expansion simulation we need to have a solid mesh to be able to capture also the shrinkage through the thickness. The solid mesh is achieved by expanding the shell mesh equally on bottom and top sides of the shell. Basically the opposite of how a shell mesh is generated from a solid mesh.

This procedure does not work for the T-beam structures. For these structures a special procedure is proposed in the paper. To capture the spring-in behavior the T-beams need to have a curved corner with radius in the transition between flange and web. Hence, a new solid three-parted mesh is created as close to the shell mesh as possible. Then the resulting displacements from the thermal expansion simulation is mapped back to the shell mesh.

### 5.2.2 Test case

A subassembly of an aircraft wing box is used to demonstrate the method proposed in Paper II. This wing box is a modified version of a case that is part

of the EU FP7 project LOCOMACHS. The subassembly consists of 15 parts, 3 of them are aluminum and the rest are composite laminae, CFRP to be more specific, see Figure 5.4. Among the composite parts there are T-beams, L-beams and C-shaped beams. Those are parts typically showing the spring-in behavior after the production process.

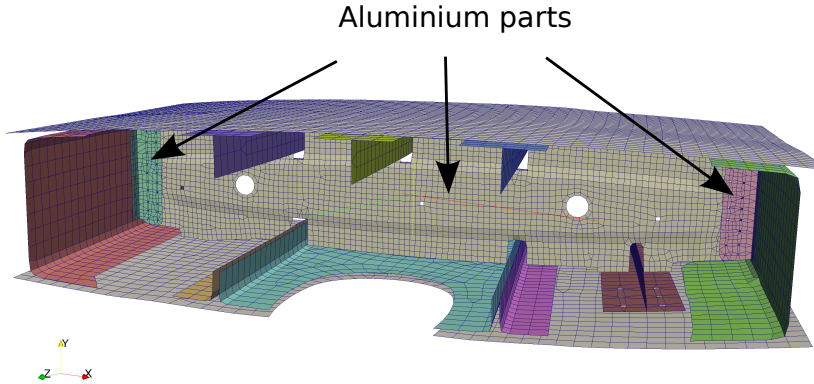


Figure 5.4: The test case used in Paper II.

The composite parts are assumed to be  $10\text{mm}$  thick and consist of three plies with equal thickness and the fiber orientations  $90^\circ/0^\circ/90^\circ$ .

As input parameters we have the curing temperature and the standard geometric parameters, locators, joining points and contact points. We assume a nominal curing temperature equal to  $120^\circ\text{C}$  and the room temperature  $20^\circ\text{C}$ , hence  $\Delta T = 100^\circ\text{C}$ . Further, the tolerance for the curing temperature is chosen such that we get the desired spring-in angle limit. In this way we capture also the chemical transition occurring during curing by adjusting the modeled parameter accordingly as done in [5, 31]. The tolerances for all parameters are stated in Table 5.2.

### 5.2.3 Results

When using the proposed method we get, for the test case, the total variation magnitude  $6\sigma_{\text{RMS}}^{\text{MAG}} = 1.36$  and in the  $y$ -direction  $6\sigma_{\text{RMS}}^{\text{Y}} = 0.83$ . With the tolerance of the curing temperature set to zero we get  $6\sigma_{\text{RMS}}^{\text{MAG}} = 0.31$  and  $6\sigma_{\text{RMS}}^{\text{Y}} = 0.14$ .

	<b>description</b>	<b>tolerance, LSL, USL at <math>\pm 3\sigma</math></b>
Process parameters	Curing temperature	$\pm 30^\circ$
	<i>Spring-in angle*</i>	$\pm 0.195^\circ$
Geometric parameters	Locators	$\pm 0.1\text{mm}$
	Joining points	0mm
	Contact points	0mm

Table 5.2: Input parameters and tolerances. \*Indirect tolerance totally dependent on the tolerance of the curing temperature.

According to these results, the total geometric variation is approximately four times larger when variation for the curing temperature is included, compared to when it is kept fixed at nominal temperature.



# Bibliography

- [1] 3DCS. On the WWW, April 2015. URL <http://www.3dcs.com>.
- [2] R. Blanc, C. Germain, J. D. costa, P. Baylou, and M. Cataldi. Fiber orientation measurements in composite materials. *Composites Part A: Applied Science and Manufacturing*, 37(2):197 – 206, 2006.
- [3] K. K. Chawla. *Composite Materials: Science and Engineering*. Springer, New York, US., 2012.
- [4] S. Dahlström and L. Lindkvist. Variation Simulation of Sheet Metal Assemblies using the Method of Influence Coefficients with Contact Modeling. *Journal of Manufacturing Science and Engineering*, 129(3):615–622, 2006.
- [5] C. Dong. *Dimension Variation Prediction and Control for Composites*. PhD Thesis, Florida State University College of Engineering, Tallahassee, FL, July 2003. See also URL <http://diginole.lib.fsu.edu/cgi/viewcontent.cgi?article=1247&context=etd>.
- [6] C. Dong, C. Zhang, Z. Liang, and B. Wang. Assembly Dimensional Variation Modelling and Optimization for the Resin Transfer Moulding Process. *Modelling Simul. Mater. Sci. Eng.*, 12(3):221–237, 2004.
- [7] R. F. Gibson. A review of recent reseach on mechanics of multifunctional composite materials and structures. *Composite Structures*, 92:2793–2810, 2010.
- [8] Goodfellow. Carbon/epoxy - sheet - material information. On the WWW, April 2015. URL <http://www.goodfellow.com/E/Carbon-Epoxy-Composite-Sheet.html>.
- [9] Gurit. Guide to composites. On the WWW, April 2015. URL <http://www.gurit.com>.

- 
- [10] Y. S. Hong and T. C. Chang. A comprehensive review of tolerancing research. *International Journal of Production Research*, 40(11):2425–2459, 2002.
- [11] T. J. R. Hughes. *The finite element method: linear static and dynamic finite element analysis*. Dover Publications, Inc., Mineola, New York, 2000.
- [12] A. Ibrahimbegović. Stress Resultant Geometrically Nonlinear Shell Theory with Drilling Rotations - Part I: A Consistent Formulation. *Methods in Applied Mechanics and Engineering*, 118:265–284, 1994.
- [13] A. Ibrahimbegović and F. Frey. Stress Resultant Geometrically Nonlinear Shell Theory with Drilling Rotations - Part III: Linearized Kinematics. *International Journal for Numerical Methods in Engineering*, 37:3659–3683, 1994.
- [14] A. Ibrahimbegović and F. Frey. Stress resultant geometrically nonlinear shell theory with drilling rotations—Part II. Computational aspects . *Computer Methods in Applied Mechanics and Engineering*, 118(3–4):285 – 308, 1994.
- [15] LaStFEM. On the WWW, April 2015. URL [www.fcc.chalmers.se/technologies/comp/computational-structural-dynamics/](http://www.fcc.chalmers.se/technologies/comp/computational-structural-dynamics/).
- [16] S. C. Liu and S. J. Hu. Variation Simulation for Deformable Sheet Metal Assemblies using Finite Element Methods. *Journal of Manufacturing Science and Engineering*, 119(3):368–374, 1997.
- [17] J. Lööf, R. Söderberg, and L. Lindkvist. Optimizing Locator Position to Maximise Robustness in Critical Product Dimension. *Proceedings of ASME 2009 IDETC/CIE*, 2:515–522, August–September 2009.
- [18] S. Lorin, C. Cromvik, F. Edelvik, L. Lindkvist, and R. Söderberg. On the robustness of the volumetric shrinkage method in the context of variation simulation. In *Proceedings of the ASME 2014 International Mechanical Engineering Congress & Exposition*, 2014.
- [19] S. Lorin, C. Cromvik, F. Edelvik, L. Lindkvist, and R. Söderberg. Variation simulation of welded assemblies using a thermo-elastic finite element model. *Journal of Computing and Information Science in Engineering*, 14, 2014.
- [20] S. Lorin, C. Cromvik, F. Edelvik, L. Lindkvist, R. Söderberg, and K. Wärmefjord. Simulation of non-nominal welds by resolving the melted zone and its implication to variation simulation. In *Proceeding of the ASME 2014 International Design Engineering Technical Conference & Computers and Information in Engineering Conference*, 2014.

- 
- [21] S. Lorin, C. Cromvik, F. Edelvik, and R. Söderberg. Welding simulation of non-nominal structures with clamps. *Journal of Computing and Information Science in Engineering*, 15, 2015.
- [22] E. Maass and P. D. McNair. *Applying design for six sigma to software and hardware systems*. Pearson Education, Inc., Boston, MA, 2009.
- [23] A. Mark, E. Svenning, R. Rundqvist, F. Edelvik, E. Glatt, S. Rief, A. Wiegmann, M. Fredlund, R. Lai, L. Martinsson, and U. Nyman. Microstructure Simulation of Early Paper Forming Using Immersed Boundary Methods. *Progress in Paper Physics Seminar*, pages 283–290, September 2011.
- [24] N. Ottosen and H. Petersson. *Introduction to the finite element method*. Prentice Hall, Harlow, England, 1992.
- [25] RD&T. On the WWW, April 2015. URL <http://www.rdnt.se>.
- [26] J. C. Simo and D. D. Fox. On a Stress Resultant Geometrically Exact Shell Model. Part I: Formulation and Optimal Parametrization. *Methods in Applied Mechanics and Engineering*, 72:267–304, 1989.
- [27] R. Söderberg, L. Lindkvist, and J. S. Carlson. Managing Physical Dependencies through Locating System Design. *Journal of Engineering Design*, 17(4):325–346, 2006.
- [28] E. Svenning, A. Mark, F. Edelvik, E. Glatt, S. Rief, A. Wiegmann, L. Martinsson, R. Lai, M. Fredlund, and U. Nyman. Multiphase simulation of fiber suspension flows using immersed boundary methods. *Nordic Pulp & Paper Research Journal*, 27(2):184–191, 2012.
- [29] VSA. On the WWW, April 2015. URL [http://www.plm.automation.siemens.com/en\\_us/products/tecnomatix/manufacturing-planning/dimensional-quality/variation-analysis.shtml](http://www.plm.automation.siemens.com/en_us/products/tecnomatix/manufacturing-planning/dimensional-quality/variation-analysis.shtml).
- [30] K. Wärmefjord, L. Lindkvist, and R. Söderberg. Tolerance Simulation of Compliant Sheet Metal Assemblies Using Automatic Node-Based Contact Detection. *Proceedings of ASME 2008 IMECE*, 14:35–44, October–November 2008.
- [31] M. Zarrelli, A. A. Skordos, and I. K. Partridge. Investigation of Cure Induced Shrinkage in Unreinforced Epoxy Resin. *Plastics, Rubber and Composites Processing and Applications*, 31(9):377–384, November 2002.

- [32] C. Zhang and H.-P. B. Wang. *Tolerancing for Design and Manufacturing*, in *Handbook of Design, Manufacturing and Automation* (eds R. C. Dorf and A. Kusiak). John Wiley & Sons, Inc., Hoboken, NJ, USA, 1994.